

## Selective alpha particle decay of $^{12}\text{C} + ^{12}\text{C}$ resonances to excited $^{20}\text{Ne}$ rotational bands observed in the $^{12}\text{C}(^{12}\text{C}, \alpha)^{20}\text{Ne}$ reaction

R. J. Ledoux, C. E. Ordoñez, M. J. Bechara,\* H. A. Al-Juwair, G. Lavelle, and E. R. Cosman

*Department of Physics and Laboratory for Nuclear Science, Massachusetts Institute of Technology, Cambridge, Massachusetts 02139*

(Received 28 March 1983; revised manuscript received 11 April 1984)

Excitation functions of the  $^{12}\text{C}(^{12}\text{C}, \alpha)^{20}\text{Ne}$  reaction were measured at  $\theta_{\text{lab}} = 7.5^\circ$  between  $E_{\text{c.m.}} = 14\text{--}40$  MeV and angular distributions were measured from  $E_{\text{c.m.}} = 17.8$  to 20.6 MeV. Summed yields reveal prominent intermediate structure resonances over the entire range which correlate well to resonances previously observed in elastic data. The resonances show enhanced decays to excited rotational bands in  $^{20}\text{Ne}$  with reduced widths comparable to those for the elastic channel and an order of magnitude greater than those for the  $^{20}\text{Ne}$  ground state band. A discussion is given of the resonances as shape-isomeric states in a shell model secondary minimum in  $^{24}\text{Mg}$ , and of the selective alpha decay as being transitions to states of related configuration in  $^{20}\text{Ne}$ .

### I. INTRODUCTION

The origin of the intermediate structure resonances seen in the  $^{12}\text{C} + ^{12}\text{C}$  system is still an outstanding problem in nuclear physics. Their first observation below the Coulomb barrier<sup>1</sup> prompted models of nuclear molecules<sup>1,2</sup> and alpha clustering.<sup>3</sup> Later they were proven to exist well above the barrier<sup>4</sup> and to decay nonstatistically in the light particle channels, indicative of specific structural information. An apparent rotational band of resonances was found<sup>5</sup> linking the sub- and above-barrier resonances, and it was suggested that the resonances might be manifestations of shape-isomeric states in  $^{24}\text{Mg}$ . Expanded studies of  $^{12}\text{C} + ^{12}\text{C}$  fusion yields,<sup>6,7</sup> inelastic scattering,<sup>8,9</sup> and reaction data<sup>10</sup> stimulated and supported other explanations for the resonances, including the following: optical model shape resonances,<sup>11</sup> resonant inelastic coupling,<sup>12,13</sup> doorway state fragmentation,<sup>14</sup> interacting boson representations,<sup>15</sup> and diffraction.<sup>16</sup> Although each of these model interpretations explains some aspects of the data, no one or combination of more than one of them has given a consistent picture of all of the data.

An aspect of the  $^{12}\text{C} + ^{12}\text{C}$  data which has slowed progress has been the difficulty in determining which anomalies in the excitation functions are intermediate structure resonances and which are statistical fluctuations. The difficulty is most severe in the region above the Coulomb barrier. Several studies, some very recent, have claimed that most of the large variations in energy in the elastic,<sup>17</sup> alpha,<sup>18,19</sup> and proton<sup>20</sup> channel excitation functions are consistent with statistical fluctuations. Other studies<sup>4,5,10,21,22</sup> have claimed that these same channels show many, true, nonoverlapping resonances. The difference between these conclusions can be traced to the selection, quantity, and detail of the data considered, the degree to which cross-channel correlations are examined, and the assumptions made in the statistical analyses of the data. In one of these works,<sup>21</sup> it was suggested that the peaks in the  $90^\circ$  c.m. elastic scattering excitation functions are a good representation of the  $^{12}\text{C} + ^{12}\text{C}$  intermediate structure resonance positions.

In this paper, a study of the excitation functions of the  $^{12}\text{C}(^{12}\text{C}, \alpha)^{20}\text{Ne}$  reaction to highly excited states in  $^{20}\text{Ne}$  is done in the range  $E_{\text{c.m.}} = 13.8\text{--}40.2$  MeV following the suggestions of Ref. 21. Preliminary results of this study have already been reported.<sup>23</sup> In Sec. II of this paper, the experimental data are shown and the  $\alpha + ^{20}\text{Ne}$  channel is correlated to the  $90^\circ$  c.m. elastic yields. Reduced widths for  $^{12}\text{C} + ^{12}\text{C}$  and  $\alpha + ^{20}\text{Ne}(i)$  decays are given for the resonances at  $E_{\text{c.m.}} = 18.4, 19.3,$  and  $20.3$  MeV. Possible relations of the present  $^{12}\text{C}(^{12}\text{C}, \alpha)^{20}\text{Ne}$  results to several model calculations and the other data are given in Sec. III. A spectroscopic explanation of the  $\alpha + ^{20}\text{Ne}^*$  decays in terms of transitions between shape-isomeric states in  $^{24}\text{Mg}^*$  and  $^{20}\text{Ne}^*$  is proposed. Evidence is presented that  $^{12}\text{C} + ^{12}\text{C}$  resonances from below to well above the Coulomb barrier all have a common origin.

### II. EXPERIMENTAL RESULTS AND ANALYSIS

The  $^{12}\text{C}(^{12}\text{C}, \alpha)^{20}\text{Ne}$  reaction was studied using the Brookhaven National Laboratory (BNL) Tandem Van de Graaff accelerators, natural carbon targets of approximate thickness  $20 \mu\text{g}/\text{cm}^2$ , and a silicon surface barrier detector telescope. Excitation functions were measured from  $E_{\text{c.m.}} = 14$  to 40 MeV in 100 keV steps. Typical alpha particle spectra are shown in Fig. 1, in which the energy resolution is between 100 and 200 keV (lab) for  $E_{\text{c.m.}} < 25$  MeV and between 200 to 300 keV (lab) for  $E_{\text{c.m.}} > 25$  MeV. The carbon targets had a thin layer of gold (less than  $1 \mu\text{g}/\text{cm}^2$ ) deposited on them, and the Rutherford scattering of  $^{12}\text{C}$  on  $^{197}\text{Au}$  was monitored by a counter to check relative beam normalization. The uncertainty in the absolute cross section normalization is approximately 30%. Detailed angular distributions were measured over a more limited range from  $E_{\text{c.m.}} = 17.8$  to 20.6 MeV in order to derive total cross sections to discrete  $^{20}\text{Ne}$  states over the resonances in that range.

Figure 2 shows the  $^{12}\text{C}(^{12}\text{C}, \alpha)^{20}\text{Ne}$  excitation functions for individual  $^{20}\text{Ne}$  final states. The transitions that have been included here are for the ground state band and for the most consistently prominent groups. The data were

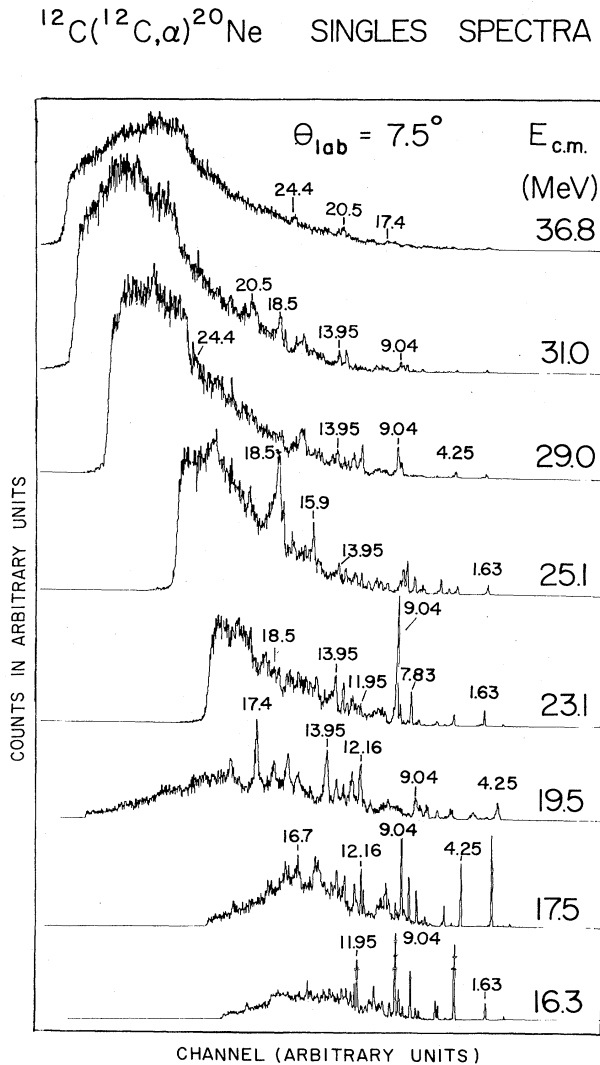


FIG. 1. Selected  $^{12}\text{C}(^{12}\text{C},\alpha)^{20}\text{Ne}$  reaction singles spectra taken with a surface barrier detector telescope at  $\theta_{\text{lab}}=7.5^\circ$ . The excitation of the states in  $^{20}\text{Ne}$  are labeled in MeV above the spectra.

taken in three experimental episodes, and the alpha telescope detectors were chosen in each energy range to span as large a range of  $E_x(^{20}\text{Ne})$  as possible. In the range of  $E_{\text{c.m.}}=18\text{--}29$  MeV, the alpha particles for the  $E_x=0.0$ , 1.63, and 4.25 MeV groups in  $^{20}\text{Ne}$  were not stopped in the telescope, so that  $\theta_{\text{lab}}=5^\circ$  data from Ref. 19 have been substituted in Fig. 2 for these transitions. All other data are from the present measurement at  $\theta_{\text{lab}}=7.5^\circ$ .

It is evident from these data that there is a distinct final state selectivity to states of high spin and excitation in  $^{20}\text{Ne}$ , their excitation functions all showing prominent structure. Although such single-angle data for a given transition do not easily show the correlated nature of the intermediate structures which lie in the region studied, the sum of the data over all states does. Figure 3 compares the sum of the data in Fig. 2 to the total alpha yields [ $^{20}\text{Ne}\rightarrow\gamma$  and  $^{16}\text{O}(3^-\rightarrow 0^+)$ ] of Kolata *et al.*,<sup>7</sup> and the  $90^\circ$  c.m. elastic data of Shapira *et al.*<sup>17</sup> The present

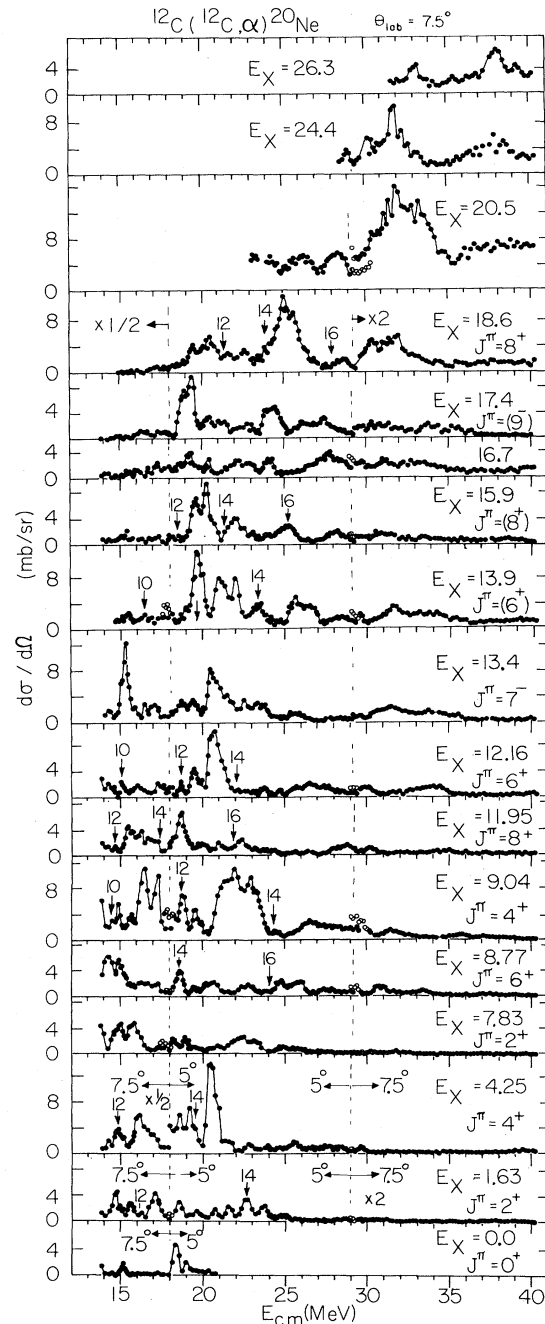


FIG. 2. Selected excitation functions of the  $^{12}\text{C}(^{12}\text{C},\alpha)^{20}\text{Ne}$  reaction at  $\theta_{\text{lab}}=7.5^\circ$ . Only the more prominent  $^{20}\text{Ne}$  transitions or those of special interest are shown. Measured and tentative (parentheses)  $J^\pi$  values are also labeled. The arrows indicate the position for the grazing energy associated with the  $l$  value indicated above them. Note the following: The  $E_x=0.0$ , 1.63, and 4.25 MeV transitions for  $E_{\text{c.m.}}=18\text{--}29$  were taken from Greenwood *et al.* (Ref. 19) since our detector did not stop these transitions at  $\theta_{\text{lab}}=7.5^\circ$ .

single-angle data and the summed-angle data of Kolata *et al.*<sup>7</sup> agree in most details, proving that the former faithfully represent the resonances.<sup>21</sup> There is also a clear, visual correlation of positions where both the alpha and the  $90^\circ$  c.m. elastic data show prominent intermediate

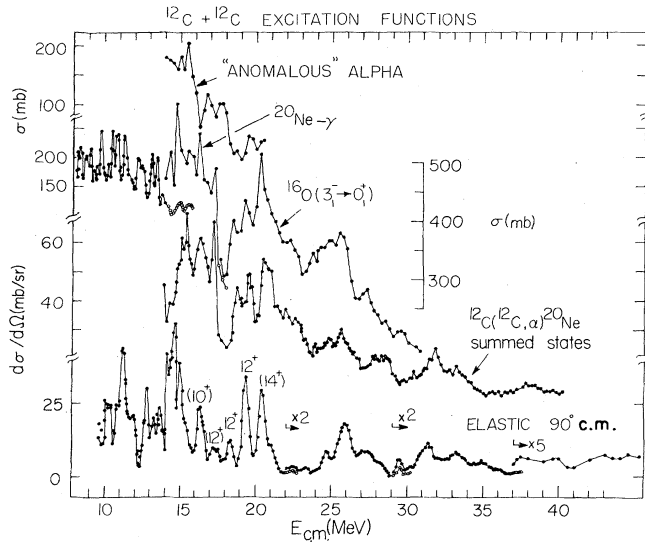


FIG. 3. Comparison of the summed  $\theta_{\text{lab}}=7.5^\circ$   $^{12}\text{C}(^{12}\text{C},\alpha)^{20}\text{Ne}^*$  excitation functions of Fig. 2 to  $^{12}\text{C}(^{12}\text{C},\alpha)^{20}\text{Ne}$  total yields from Kolata *et al.* (Ref. 7) and to  $^{12}\text{C}+^{12}\text{C}$   $90^\circ$  (c.m.) elastic excitation functions (Ref. 17). See the text for other details.

structures, especially in the vicinity of  $E_{\text{c.m.}}=20, 25,$  and  $30$  MeV. The correlation function of the  $90^\circ$  c.m. elastic data with the summed  $7.5^\circ$  laboratory alpha data is shown in Fig. 4. Its positive character suggests that the  $90^\circ$  c.m. elastic scattering in the region is a direct indicator of the resonance positions.

The selected angular distributions and angle-integrated cross sections measured in detail over the interesting range of  $E_{\text{c.m.}}=17.8\text{--}20.6$  MeV (where there are very prominent resonances present, as can be seen in Fig. 3) are shown in Figs. 5 and 6, respectively. To demonstrate more quantitatively the nonstatistical character of the  $\alpha+^{20}\text{Ne}^*$  decays, the angle-integrated yields are used to extract reduced widths for three of the most prominent resonances at  $E_{\text{c.m.}}=18.4, 19.3,$  and  $20.3$  MeV. To do this, the purely resonant part of the cross section  $\sigma_{\text{res}}(i, E_{\text{c.m.}})$ , at the resonant energy  $E_{\text{c.m.}}$  for a given final state  $^{20}\text{Ne}^*(i)$ , is extracted by subtracting from the observed on-resonance cross section  $\sigma_{\text{exp}}(i, E_{\text{c.m.}})$  a smooth

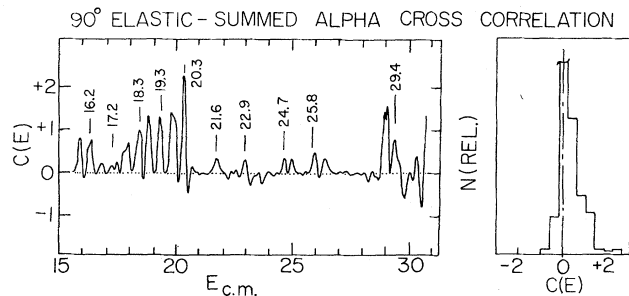


FIG. 4. Correlation function between the  $^{12}\text{C}+^{12}\text{C}$   $90^\circ$  (c.m.) elastic channel and the summed  $^{12}\text{C}(^{12}\text{C},\alpha)^{20}\text{Ne}$   $\theta=7.5^\circ$  (lab) reaction data of the present work.

background cross section  $\sigma_{\text{bkd}}(i, E_{\text{c.m.}})$  deduced from cross sections off resonance. Then, for nonoverlapping resonances,

$$\begin{aligned} \sigma_{\text{res}}(i, E_{\text{c.m.}}) &= \sigma_{\text{exp}}(i, E_{\text{c.m.}}) - \sigma_{\text{bkd}}(i, E_{\text{c.m.}}) \\ &= 8\pi\lambda^2(2l+1) \frac{\Gamma_{\text{el}}(^{12}\text{C})\Gamma_{\alpha}(i)}{\Gamma_{\text{tot}}^2}, \end{aligned} \quad (1)$$

where  $\Gamma_{\text{el}}(^{12}\text{C})$  is the elastic partial width,  $\Gamma_{\alpha}(i)$  is the  $\alpha+^{20}\text{Ne}^*(i)$  partial width, and  $\Gamma_{\text{tot}}$  is the total width.  $\Gamma_{\text{el}}(^{12}\text{C})$  and  $\Gamma_{\text{tot}}$  for each resonance are deduced from elastic scattering fits.<sup>8,21,23,24</sup> They are somewhat dependent on the assumed  $J^\pi$  values for the resonances but variation of  $\pm 2\hbar$  in these  $J^\pi$  values is seen to not affect the calculated reduced widths appreciably. To estimate the  $\alpha+^{20}\text{Ne}^*(i)$  reduced widths it is assumed that

$$\Gamma_{\alpha}(i) = \Gamma_{\alpha}^l(i), \quad (2)$$

where  $l = J_{\text{res}} - J_i$  is the minimum angular momentum between the resonance and the final state. The alpha reduced widths are then approximated as

$$\gamma_{\alpha}^2(i) = \frac{\Gamma_{\alpha}(i)}{2P_{\alpha l}(i)}, \quad (3)$$

where  $P_{\alpha l}(i)$  is the Coulomb penetration factor for an alpha particle of angular momentum  $l$  emitted to the final state  $^{20}\text{Ne}^*(i)$ . The ratio of the reduced width to the Wigner limit is given by

$$\theta^2(i) = \frac{\gamma_{\alpha}^2(i)}{\gamma_w^2}, \quad (4)$$

where

$$\gamma_w^2 = \frac{3}{2} \frac{\hbar^2}{\mu R^2}, \quad (5)$$

$\mu$  and  $R$  being the  $\alpha+^{20}\text{Ne}$  reduced mass and channel radius, respectively. The reduced widths and their ratios to the Wigner limit, for transitions included in Fig. 2, are summarized in Tables I–IV.

As is evident from Eqs. (1)–(3), the alpha reduced widths  $\gamma_{\alpha}^2$  are dependent on  $\Gamma_{\text{el}}(^{12}\text{C})$ ,  $\Gamma_{\text{tot}}$ , and  $J_{\text{res}}^\pi$ . For this analysis, these quantities were obtained from a phase shift analysis of the elastic scattering angular distributions,<sup>24</sup> where values of  $J^\pi=12^+, 12^+,$  and  $(12^+, 14^+)$  have been obtained for the resonances at  $E_{\text{c.m.}}=18.4, 19.3,$  and  $20.3$  MeV, respectively. Reduced widths for the  $20.3$  MeV resonance were calculated assuming both  $J^\pi=12^+$  (Table III), and  $J^\pi=14^+$  (Table IV).

Two different channel radii ( $R=5.38$  and  $6.02$  fm) were used in the calculations, and it is seen that the absolute value of the reduced width is strongly dependent on the channel radius. However, it is important to note that the ratio of the reduced width to the Wigner limit for different transitions is not strongly dependent on the channel radius. Therefore, statements about selectivity are relatively independent of the channel radius used to extract reduced widths.

The main source of error in the reduced widths comes from uncertainties in the resonant cross sections  $\sigma_{\text{res}}(i, E_{\text{c.m.}})$  due to difficulties in estimating the non-

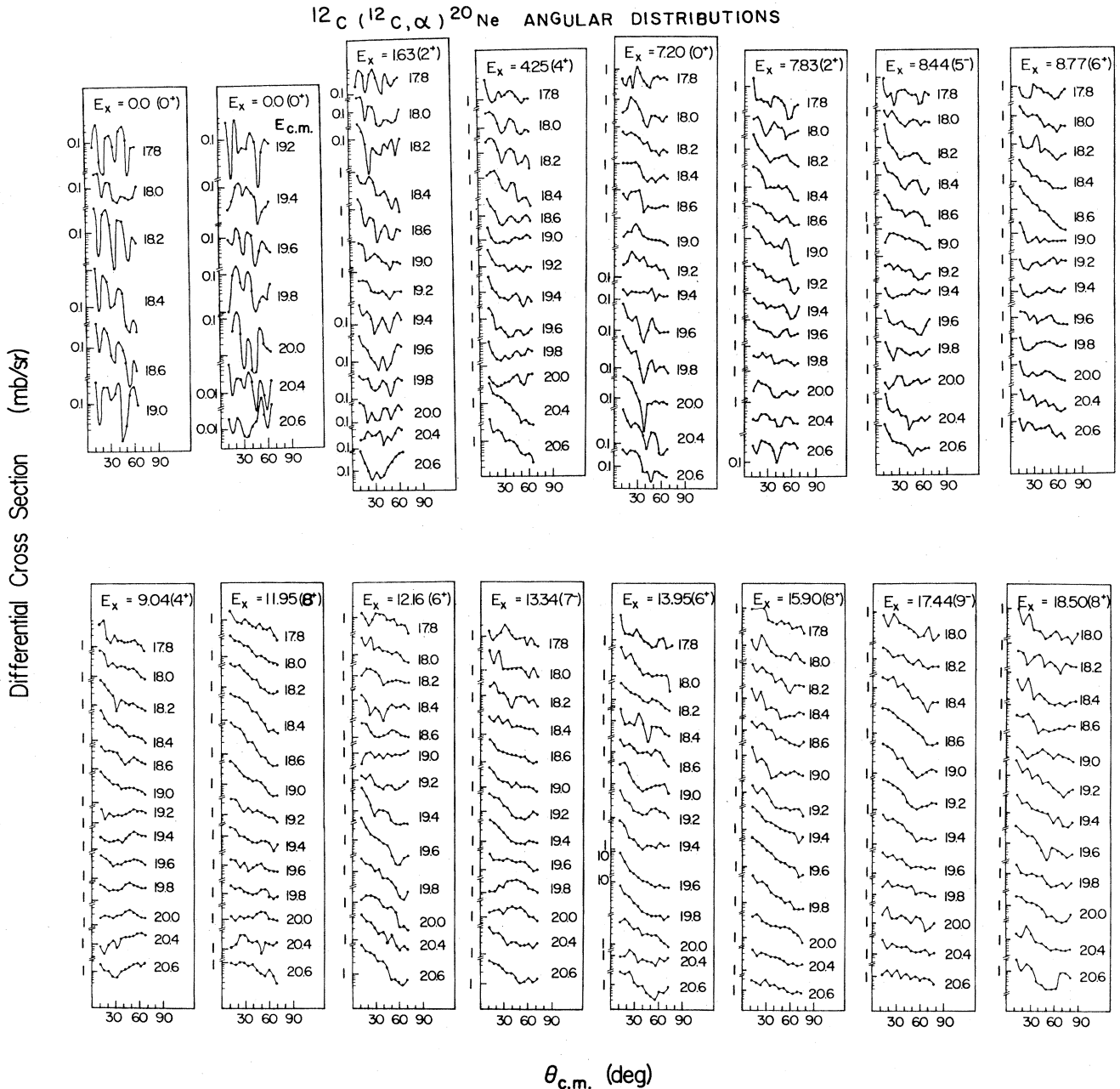


FIG. 5. Angular distributions of selected  $^{12}\text{C}(^{12}\text{C}, \alpha)^{20}\text{Ne}$  transitions between  $E_{\text{c.m.}} = 17.8$  and  $20.6$  MeV.

resonant background  $\alpha_{\text{bkd}}(i, E_{\text{c.m.}})$  of the excitation functions in Fig. 6. The extracted resonant cross sections are on the average accurate to the 50% level. It is particularly difficult to extract resonant cross sections for transitions with weak resonant decay strengths. For these transitions, only upper limits for the reduced widths have been calculated. States for which upper limits have been calculated have been bracketed in Tables I–IV.

We note that the widths given in Tables I, II, and IV together with other reaction data are consistent with limits imposed by unitarity. This result is summarized in

Table V. For example, considering the  $E_{\text{c.m.}} = 19.3$  MeV resonance, with  $\Gamma_{\text{el}} = 80$  keV, and  $\Gamma_{\text{tot}} = 400$  keV from Ref. 24, and using the total inelastic excitation functions for Cormier *et al.*,<sup>8</sup> one can calculate the total inelastic width  $\Gamma_{\text{inel}} = 125$  keV. Furthermore, by adding up the individual alpha widths  $\Gamma_{\alpha}(i)$  in Table II, one gets an estimated total alpha width for the 19.3 MeV resonance of  $\Gamma_{\alpha} = 207$  keV. As pointed out in Sec. III below, this sum of  $\Gamma_{\alpha}(i)$  for the prominent  $\alpha + ^{20}\text{Ne}^*(i)$  transitions seen here must nearly exhaust the full alpha decay width, so that this is a reasonable approximation. Summing these

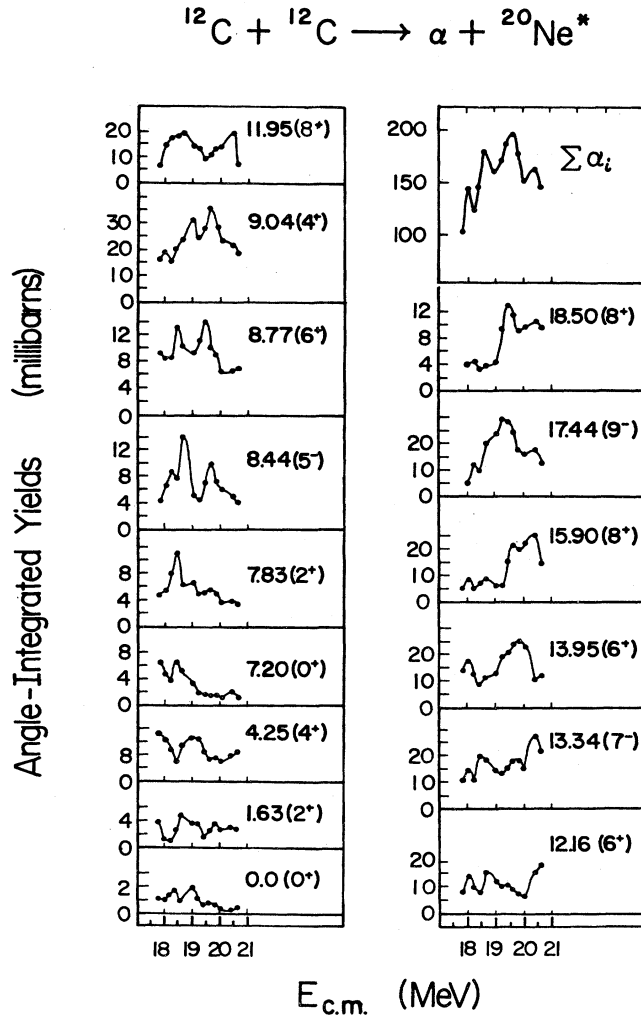


FIG. 6. Angle-integrated excitation functions of selected  $^{12}\text{C}(^{12}\text{C},\alpha)^{20}\text{Ne}$  transitions.

widths we get,

$$\Gamma_{\text{tot}}(\text{calc}) = \Gamma_{\text{el}}(^{12}\text{C}) + \Gamma_{\text{inel}} + \Gamma_{\alpha} = 412 \text{ keV}. \quad (6)$$

This is close to the  $\Gamma_{\text{tot}} = 400 \text{ keV}$  from Ref. 24, and is thus consistent with the experimentally observed fact<sup>7</sup> that the elastic, inelastic, and alpha channels exhaust most of the resonant width. Furthermore, Kolata *et al.*<sup>7</sup> have measured the resonant total cross sections for all prominent reaction channels. Subtracting appropriate non-resonant backgrounds and summing the resonant partial cross sections from Ref. 7, one obtains a total resonant cross section of  $\sigma_{\text{res}}^{\text{tot}}(\text{exp}) = 185 \text{ mb}$ . Then, using

$$\frac{\Gamma_{\text{el}}(^{12}\text{C})}{\Gamma_{\text{tot}}} = 0.2$$

from Ref. 24, one calculates

$$\begin{aligned} \sigma_{\text{res}}^{\text{tot}}(\text{calc}) &= 8\pi\lambda^2(2l+1) \frac{\Gamma_{\text{el}}(^{12}\text{C})[\Gamma_{\text{tot}} - \Gamma_{\text{el}}(^{12}\text{C})]}{\Gamma_{\text{tot}}^2} \\ &= 180 \text{ mb}. \end{aligned} \quad (7)$$

This agreement again suggests that the widths used here are reasonable. Similarly calculated values for the  $E_{\text{c.m.}} = 18.4(12^+)$  and  $20.3(14^+)$  MeV resonances are also given in Table V.

### III. DISCUSSION

In this section we shall first make some general observations on the present results and then compare our data to several pertinent theoretical and experimental studies.

A striking feature of the results shown in Tables I–IV is the highly nonstatistical nature of the alpha decays from the  $E_{\text{c.m.}} = 18.4, 19.3,$  and  $20.3 \text{ MeV}$  resonances to excited rotational band levels in  $^{20}\text{Ne}$ , once the latter are above threshold. The reduced widths for transitions to the selected excited  $^{20}\text{Ne}$  states, most of which are thought

TABLE I. Reduced widths for selected final states of the  $^{12}\text{C}(^{12}\text{C},\alpha)^{20}\text{Ne}$  reaction. All widths are in keV and all cross sections in mb.  $E_{\text{c.m.}}(^{12}\text{C}) = 18.4 \text{ MeV}$ ,  $J^{\pi} = 12^+$ ,  $\Gamma_{\text{el}}(^{12}\text{C})/\Gamma_{\text{tot}} = 0.13$ ,  $\Gamma_{\text{tot}} = 400.0 \text{ keV}$ .

$E_x(^{20}\text{Ne})$ (MeV)	$J^{\pi}$	$\sigma_{\text{res}}(i)$	$\Gamma_{\alpha}(i)$	$\gamma^{2a}$	$\theta^2$ (%)	$\gamma^{2b}$	$\theta^2$ (%)
0.0	$0^+$	1.8	4.6	42.0	6.4	6.4	1.2
1.63	$2^+$	2.7	7.0	9.1	1.4	2.6	0.5
4.25	$4^+$	2.0	5.3	2.4	0.4	1.1	0.2
8.77	$6^+$	7.0	18.4	8.2	1.3	4.1	0.8
11.95	$8^+$	12.0	31.5	13.0	2.0	7.4	1.4
7.20	$0^+$	5.0	13.1	12 600.0	[1931.0]	1100.0	[213.0]
7.83	$2^+$	8.0	21.0	773.0	119.0	116.0	22.3
8.44	$5^-$	4.5	11.8	11.0	1.6	4.1	0.8
9.04	$4^+$	5.0	13.1	52.0	8.0	13.2	2.6
12.16	$6^+$	3.0	7.9	21.0	3.3	6.8	1.3
13.34	$7^-$	10.0	26.3	57.0	8.7	20.6	4.0
13.95	$6^+$	1.0	2.6	36.0	5.6	9.2	1.8
15.9	$8^+$	2.0	5.3	53.0	8.1	16.5	3.2
17.44	$9^-$	5.0	13.1	522.0	80.3	156.0	30.1
18.5	$8^+$	1.0	2.6	6293.0	[967.4]	1410.0	[272.0]

<sup>a</sup> $\alpha + ^{20}\text{Ne}$  channel radius = 5.38 fm,  $\gamma_w^2$  (Wigner limit for  $\alpha + ^{20}\text{Ne}$  channel) = 650 keV.

<sup>b</sup> $\alpha + ^{20}\text{Ne}$  channel radius = 6.02 fm,  $\gamma_w^2 = 519 \text{ keV}$ .

TABLE II. Reduced widths for selected final states of the  $^{12}\text{C}(^{12}\text{C},\alpha)^{20}\text{Ne}$  reaction. All widths are in keV and all cross sections in mb.  $E_{\text{c.m.}}(^{12}\text{C})=19.3$  MeV,  $J^\pi=12^+$ ,  $\Gamma_{\text{el}}(^{12}\text{C})/\Gamma_{\text{tot}}=0.02$ ,  $\Gamma_{\text{tot}}=400.0$  keV.

$E_x(^{20}\text{Ne})$ (MeV)	$J^\pi$	$\sigma_{\text{res}}(i)$	$\Gamma_\alpha(i)$	$\gamma^{2a}$	$\theta^2$ (%)	$\gamma^{2b}$	$\theta^2$ (%)
0.0	0 <sup>+</sup>	1.0	1.8	10.9	1.7	1.8	0.3
1.63	2 <sup>+</sup>	3.0	5.4	5.1	0.8	1.6	0.3
4.25	4 <sup>+</sup>	6.0	10.8	3.9	0.6	1.8	0.4
8.77	6 <sup>+</sup>	8.0	14.4	4.8	0.7	2.6	0.5
11.95	8 <sup>+</sup>	7.5	13.5	4.1	0.6	2.5	0.5
7.20	0 <sup>+</sup>	1.0	1.8	810.0	[125.0]	76.0	[15.0]
7.83	2 <sup>+</sup>	2.5	4.5	87.0	13.0	14.0	2.7
8.44	5 <sup>-</sup>	6.0	10.8	6.7	1.0	2.8	0.5
9.04	4 <sup>+</sup>	15.0	27.0	63.0	9.6	18.0	3.4
12.16	6 <sup>+</sup>	5.0	9.0	13.0	2.0	4.8	0.9
13.34	7 <sup>-</sup>	5.0	9.0	10.0	1.6	4.2	0.8
13.95	6 <sup>+</sup>	13.0	23.0	130.0	20.0	37.0	7.2
15.9	8 <sup>+</sup>	10.0	18.0	61.0	9.4	22.0	4.3
17.44	9 <sup>-</sup>	25.0	45.0	371.0	57.0	127.0	25.0
18.5	8 <sup>+</sup>	7.0	13.0	2670.0	410.0	660.0	130.0

<sup>a</sup> $\alpha+^{20}\text{Ne}$  channel radius = 5.38 fm,  $\gamma_w^2$  (Wigner limit for  $\alpha+^{20}\text{Ne}$  channel) = 650 keV.

<sup>b</sup> $\alpha+^{20}\text{Ne}$  channel radius = 6.02 fm,  $\gamma_w^2 = 519$  keV.

to be members of 8p-4h excited rotational bands,<sup>29,30</sup> exceed those for transitions to members of the ground state rotational band by about an order of magnitude. The decays are nonstatistical since, if they followed penetration factors, they should strongly favor decays to lower excited states of a given  $J$  as was first pointed out by Middleton *et al.*,<sup>29</sup> and clearly demonstrated by the Hauser-Feshbach calculations for this reaction performed by Greenwood *et al.*<sup>19</sup> The departures are far greater than the experimental and calculational uncertainties, and hence, cannot come from the latter.

This result points to a greater structural parentage of

the  $^{12}\text{C}+^{12}\text{C}$  resonances to the excited rotational band states of  $^{20}\text{Ne}$  than to the ground band states of  $^{20}\text{Ne}$ , and suggests the importance of special  $\alpha+^{20}\text{Ne}^*$  configurations to an understanding of the origin of the intermediate structure resonances. Furthermore, the reduced widths for the alpha transitions from the  $^{12}\text{C}_0+^{12}\text{C}_0$  resonances to the members of the assumed excited rotational bands in  $^{20}\text{Ne}$  are of the order of 1–6%. These are comparable to the  $^{12}\text{C}_0+^{12}\text{C}_0$  elastic reduced widths factors of 12% and 7% for the 19.3 and 20.3 MeV resonances,<sup>24</sup> respectively. Similar values would pertain to the inelastic decays seen by Cormier *et al.*<sup>8</sup> This suggests the comparable impor-

TABLE III. Reduced widths for selected final states of the  $^{12}\text{C}(^{12}\text{C},\alpha)^{20}\text{Ne}$  reaction. All widths are in keV and all cross sections in mb.  $E_{\text{c.m.}}(^{12}\text{C})=20.3$  MeV,  $J^\pi=12^+$ ,  $\Gamma_{\text{el}}(^{12}\text{C})/\Gamma_{\text{tot}}=0.16$ ,  $\Gamma_{\text{tot}}=400.0$  keV.

$E_x(^{20}\text{Ne})$ (MeV)	$J^\pi$	$\sigma_{\text{res}}(i)$	$\Gamma_\alpha(i)$	$\gamma^{2a}$	$\theta^2$ (%)	$\gamma^{2b}$	$\theta^2$ (%)
0.0	0 <sup>+</sup>	0.2	0.5	1.8	0.3	0.3	0.06
1.63	2 <sup>+</sup>	3.0	6.9	4.8	0.7	1.6	0.3
4.25	4 <sup>+</sup>	4.0	9.2	2.6	0.4	1.3	0.3
8.77	6 <sup>+</sup>	1.0	2.3	0.6	0.1	0.3	0.07
11.95	8 <sup>+</sup>	14.0	32.0	7.3	1.1	4.7	0.9
7.20	0 <sup>+</sup>	1.0	2.3	480.0	[73.0]	48.0	[9.2]
7.83	2 <sup>+</sup>	1.0	2.3	23.0	3.6	4.2	0.8
8.44	5 <sup>-</sup>	1.0	2.3	1.0	0.2	0.5	0.09
9.04	4 <sup>+</sup>	6.0	14.0	19.0	2.9	6.1	1.2
12.16	6 <sup>+</sup>	10.0	23.0	19.0	2.9	8.0	1.5
13.34	7 <sup>-</sup>	17.5	40.0	26.0	4.0	12.0	2.4
13.95	6 <sup>+</sup>	3.0	6.9	17.0	2.6	5.6	1.1
15.9	8 <sup>+</sup>	20.0	46.0	63.0	9.7	27.0	5.1
17.44	9 <sup>-</sup>	12.5	29.0	67.0	10.0	27.0	5.2
18.5	8 <sup>+</sup>	6.0	14.0	400.0	62.0	113.0	22.0

<sup>a</sup> $\alpha+^{20}\text{Ne}$  channel radius = 5.38 fm,  $\gamma_w^2$  (Wigner limit for  $\alpha+^{20}\text{Ne}$  channel) = 650 keV.

<sup>b</sup> $\alpha+^{20}\text{Ne}$  channel radius = 6.02 fm,  $\gamma_w^2 = 519$  keV.

TABLE IV. Reduced widths for selected final states of the  $^{12}\text{C}(^{12}\text{C},\alpha)^{20}\text{Ne}$  reaction. All widths are in keV and all cross sections in mb.  $E_{\text{c.m.}}(^{12}\text{C})=20.3$  MeV,  $J^\pi=14^+$ ,  $\Gamma_{\text{el}}(^{12}\text{C})/\Gamma_{\text{tot}}=0.14$ ,  $\Gamma_{\text{tot}}=300$  keV.

$E_x(^{20}\text{Ne})$ (MeV)	$J^\pi$	$\sigma_{\text{res}}(i)$	$\Gamma_\alpha(i)$	$\gamma^{2a}$	$\theta^2$ (%)	$\gamma^{2b}$	$\theta^2$ (%)
0.0	0 <sup>+</sup>	0.2	0.3	31.0	4.8	2.7	0.5
1.63	2 <sup>+</sup>	3.0	5.1	41.0	6.2	6.3	1.2
4.25	4 <sup>+</sup>	4.0	6.8	12.0	1.8	3.0	0.6
8.77	6 <sup>+</sup>	1.0	1.7	2.1	0.3	0.7	0.1
11.95	8 <sup>+</sup>	14.0	24.0	18.0	2.8	7.6	1.5
7.20	0 <sup>+</sup>	0.5	0.8	$1.1 \times 10^4$	[1700.0]	650.0	[120.0]
7.83	2 <sup>+</sup>	1.0	1.7	570.0	[87.0]	54.0	[10.0]
8.44	5 <sup>-</sup>	1.0	1.7	5.9	0.9	1.4	0.3
9.04	4 <sup>+</sup>	6.0	10.0	230.0	35.0	36.0	7.0
12.16	6 <sup>+</sup>	10.0	17.0	160.0	24.0	35.0	6.7
13.34	7 <sup>-</sup>	17.5	30.0	165.0	25.0	43.0	8.3
13.95	6 <sup>+</sup>	3.0	1.7	230.0	36.0	42.0	8.1
15.9	8 <sup>+</sup>	20.0	34.0	490.0	76.0	120.0	24.0
17.44	9 <sup>-</sup>	12.5	21.0	490.0	75.0	130.0	25.0
18.5	8 <sup>+</sup>	6.0	10.0	7500.0	1100.0	1400.0	270.0

<sup>a</sup> $\alpha + ^{20}\text{Ne}$  channel radius = 5.38 fm,  $\gamma_w^2$  (Wigner limit for  $\alpha + ^{20}\text{Ne}$  channel) = 650 keV.

<sup>b</sup> $\alpha + ^{20}\text{Ne}$  channel radius = 6.02 fm,  $\gamma_w^2 = 519$  keV.

tance of the  $\alpha + ^{20}\text{Ne}^*$  excited band configurations and the  $^{12}\text{C} + ^{12}\text{C}$  configurations in a full description of the resonant  $^{24}\text{Mg}$  states.

The present data indicate that a necessary, but not sufficient, condition for an alpha transition to be prominent on resonance is that the grazing condition be approximated. This is shown in Fig. 2 by the positions of the grazing condition  $l$  values (arrows) above the excitation functions. Exceptions to this exist in the data for some cases where the grazing condition is met, but the yields are not as great as for the states in Tables I–IV. Excitation functions for these weaker decays are not shown in Fig. 2, but they include, for example, the states at  $E_x(J^\pi) = 9.99(4^+)$ ,  $15.2(6^+)$ , and  $17.3(8^+)$  MeV, two of which are shown in Ref. 19. This would suggest that the alpha particle is emitted in a peripheral fashion from the  $^{24}\text{Mg}$  resonant state and that a structural connection exists between the  $^{24}\text{Mg}$  resonances and specific  $^{20}\text{Ne}^*$  states, beyond the requirement of grazing, to produce the selected alpha transitions between them. Previous data on  $^{12}\text{C} + ^{12}\text{C}$  resonances with  $J^\pi = 2^+$  and  $4^+$  near the Coulomb barrier

also have strongly favored alpha decay to the same excited rotational bands in  $^{20}\text{Ne}$ ,<sup>31</sup> specifically to the assumed  $0^+$  and  $2^+$  lowest band members at  $E_x(^{20}\text{Ne}) = 6.72(0^+)$ ,  $7.20(0^+)$ ,  $7.43(2^+)$ , and  $7.83(2^+)$ . Thus, it may be argued that all the  $^{12}\text{C} + ^{12}\text{C}$  intermediate structure resonances have a common origin manifested by the nonstatistical alpha decays.

Most of the theoretical calculations which have been attempted to explain the  $^{12}\text{C} + ^{12}\text{C}$  resonances have not included predictions about the  $\alpha + ^{20}\text{Ne}$  decay channel and thus cannot be readily compared to the present results. For example, the quasimolecular calculations involving the shape resonance model,<sup>11</sup> band-crossing and double-resonance model,<sup>12,13</sup> and the interacting boson model<sup>15</sup> have, to date, included only the properties of the  $^{12}\text{C} + ^{12}\text{C}$  elastic and inelastic channels, and have predicted no results for the  $^{12}\text{C}(^{12}\text{C},\alpha)^{20}\text{Ne}$  reaction, *per se*. However, several reported calculations using the deformed shell model<sup>26,27</sup> and two-center shell model<sup>25,28</sup> have produced predictions which are pertinent to the resonant  $^{12}\text{C}(^{12}\text{C},\alpha)^{20}\text{Ne}$  reaction. Therefore, a brief discussion will

TABLE V. Comparison of calculated and measured total widths (in keV) and total reaction cross sections (in mb) (note all quantities are accurate to approximately the 30% level).

$E_{\text{c.m.}}^{\text{res}}$	$J^\pi$ <sup>a</sup>	$\Gamma_{\text{el}}(^{12}\text{C})$ <sup>a</sup>	$\Gamma_{\text{inel}}^{\text{c}}$	$\Gamma_\alpha^{\text{b}}$	$\Gamma_{\text{tot}}^{\text{a}}$	$\Gamma_{\text{tot}}(\text{calc})^{\text{d}}$	$\sigma_{\text{res}}^{\text{tot}}(\text{calc})^{\text{e}}$	$\sigma_{\text{res}}^{\text{tot}}(\text{exp})^{\text{f}}$
18.4	12 <sup>+</sup>	52	144	184	400	380	135	165
19.3	12 <sup>+</sup>	80	125	207	400	412	180	185
20.4	(14 <sup>+</sup> )	42	52	166	300	260	150	200

<sup>a</sup>Reference 24.

<sup>b</sup>Values from Tables I, II, and IV.

<sup>c</sup>Reference 8.

<sup>d</sup>Equation (6) in the text.

<sup>e</sup>Equation (7) in the text.

<sup>f</sup>Reference 7.

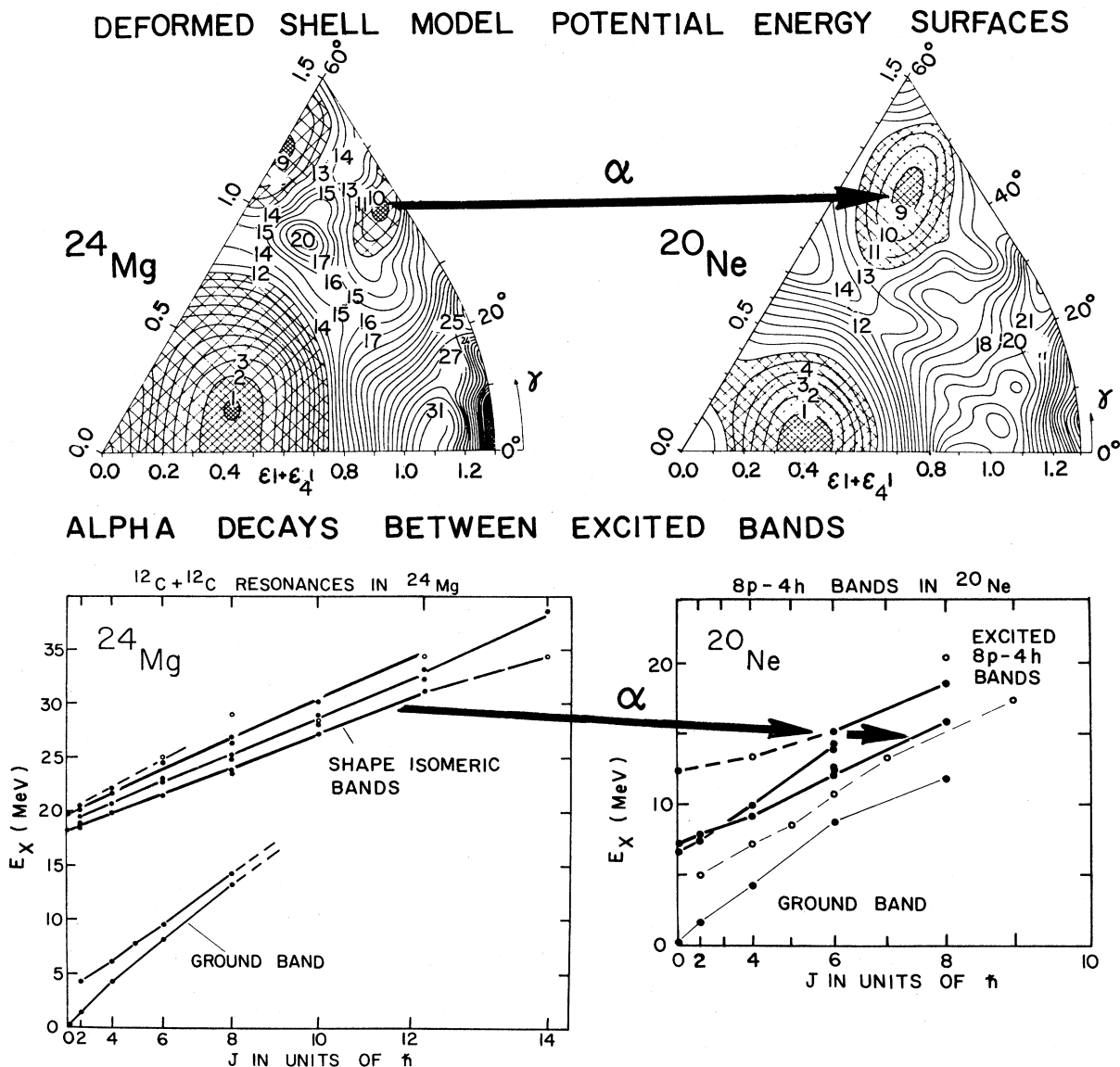


FIG. 7. Top: Potential energy surfaces at  $^{24}\text{Mg}$  as calculated from the deformed shell model (Leander and Larsson, Ref. 26). Bottom: A schematic explanation of the resonant  $^{12}\text{C}(^{12}\text{C},\alpha)^{20}\text{Ne}$  transitions as  $\alpha$  transitions between shape-isomeric configurations.

now be given of these calculations' results and how they may relate to the present data.

Leander and Larsson,<sup>26</sup> using the Nilsson model, have calculated the potential energy surfaces as a function of deformation for  $^{24}\text{Mg}$  and  $^{20}\text{Ne}$ . The calculated results, shown in Fig. 7, indicate that both nuclei have "stable" axially asymmetric minima at about the same shape (shown with the alpha decay connecting them). They state that the configuration in the axially asymmetric minimum in  $^{24}\text{Mg}$  has a  $12p-4h$  structure relative to  $^{16}\text{O}$  with a  $(2p,2n)^1$  structure in the  $(0f,1p)$  shell, a  $(2p,2n)^2$  structure in the  $(0d,1s)$  shell, and a  $(2p,2n)^{-1}$  structure in the  $(0p)$  shell.<sup>25</sup> In the notation of Arima *et al.*,<sup>32</sup> this would be  $[211]$ .

Chandra and Mosel<sup>25</sup> and Mosel<sup>28</sup> also have performed a deformed two-center shell model calculation and predict

a secondary minimum in the  $^{24}\text{Mg}$  potential energy surface. They state explicitly that it has a  $(f_{7/2})^4(p)^{-4}$  configuration (i.e.,  $[221]$ ), and relate it to the above-mentioned triaxial configuration of Leander and Larsson.<sup>26</sup> They further state that it is specifically this configuration which should have large  $^{12}\text{C}+^{12}\text{C}$ ,  $^{12}\text{C}+^{12}\text{C}^*(2^+)$ , and  $^{12}\text{C}^*(2^+)+^{12}\text{C}^*(2^+)$  widths, consistent with the elastic width estimates of Cosman *et al.*<sup>21</sup> and the inelastic data of Cormier *et al.*<sup>8</sup>

Ragnarsson *et al.*<sup>27</sup> have done a calculation similar to Leander and Larsson,<sup>26</sup> but including the effects of rotation. Specifically, they calculated the energy as a function of  $J^\pi$  for the same triaxial  $^{24}\text{Mg}$  state corresponding to that of Leander and Larsson<sup>26</sup> and Chandra and Mosel<sup>25</sup> (i.e.,  $[221]$ ). Their result is shown by the solid line in Fig. 8, and it is seen to be close to the centroids of the groups



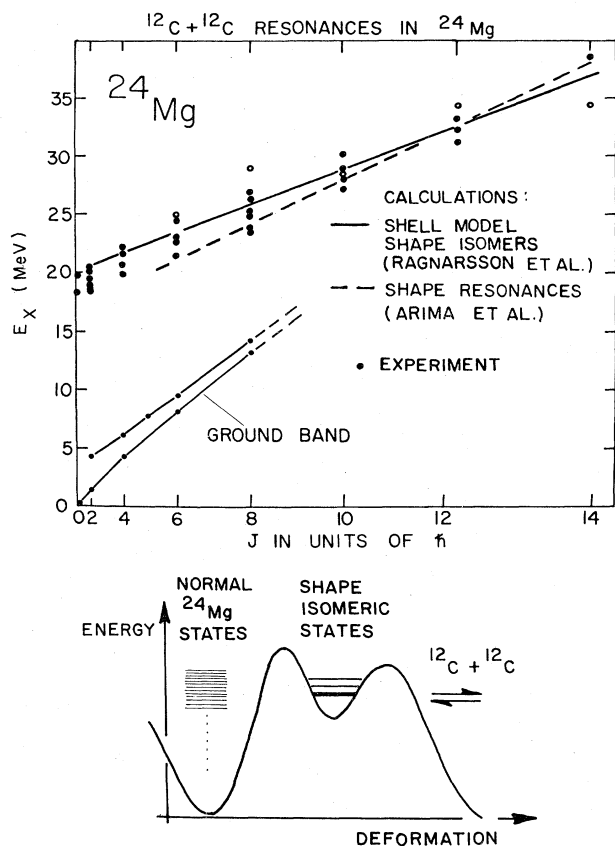


FIG. 8. A comparison of the position of known  $^{12}\text{C} + ^{12}\text{C}$  resonances in  $^{24}\text{Mg}$  and the calculated rotation sequences of the shape isomer as predicted by Ragnarsson *et al.* (Ref. 27) and shape-resonance models of Arima, Scharff-Goldhaber, and McVoy (Ref. 11).

of  $J$  states over the entire range from the Coulomb barrier,  $E_x = 20$  MeV and  $J^\pi = 0^+$ , to  $E_x = 37$  MeV and  $J^\pi = 14^+$ . This supports the view that the  $^{12}\text{C} + ^{12}\text{C}$  resonances might be  $^{24}\text{Mg}$  shape-isomeric states. The continuous trend of the resonances over this range also suggests that they have the same origin throughout. Thus, one can hypothesize that the broad grouping of  $^{12}\text{C} + ^{12}\text{C}$  resonances is a gross structure resonance, or shape resonance, that represents the virtual deformed shell model state of Ragnarsson *et al.*<sup>27</sup> Its fragmentation into intermediate structure resonances represents coupling to other degrees of freedom related to the shape isomer, viz., collective vibrations or particle-hole excitations. The intermediate structures are the eigenstates in the secondary shell model potential. They derive their enhanced  $^{12}\text{C} + ^{12}\text{C}$  widths, or quasimolecular character, from their component of the gross structure, which has strong elastic and inelastic channel coupling according to Chandra and Mosel's calculation.<sup>25,26</sup> The eigenstates are fewer in number than the ordinary states in  $^{24}\text{Mg}$  and are relatively unbroadened by the latter due to the potential barrier between them.

The shape isomer picture also provides a plausible spectroscopic explanation for the enhanced  $^{12}\text{C}(^{12}\text{C}, \alpha)^{20}\text{Ne}^*$  transitions to excited  $^{20}\text{Ne}$  bands observed here. Leander

and Larsson<sup>26</sup> have shown that the triaxial secondary minimum of  $^{20}\text{Ne}$  shown in Fig. 7 corresponds to an 8p-4h state relative to  $^{16}\text{O}$ , and mention that the  $E_x = 7.2$  MeV state is a likely candidate for such a state. They state that its configurations would be a  $(2p, 2n)^2$  structure in the  $(0d, 1s)$  shell and a  $(2p, 2n)^{-1}$  structure in the  $(0p)$  shell, i.e., [220] in the notation of Arima *et al.*<sup>32</sup> In  $^{20}\text{Ne}$  it is expected that the 8p-4h states, which include [220] and [211] states and their associated band numbers, should have enhanced  $\alpha$  decay from the band members associated with 12p-4h or [221] band heads in  $^{24}\text{Mg}$ , illustrated in Fig. 9. Middleton *et al.*,<sup>29</sup> Greenwood *et al.*,<sup>19</sup> and Hindi *et al.*<sup>30</sup> all suggest the  $E_x = 7.2$  MeV state in  $^{20}\text{Ne}$  to be 8p-4h [220], and propose the associated rotational band to be the following:  $E_x(J^\pi) = 7.20(0^+)$ ,  $7.83(2^+)$ ,  $9.04(4^+)$ ,  $12.16(6^+)$ , and  $15.9(8^+)$  MeV. These  $K^\pi = 0_3^+$  band members are connected by a heavy solid line in Fig. 7. From the present  $^{12}\text{C}(^{12}\text{C}, \alpha)^{20}\text{Ne}$  data, they all show nonstatistically enhanced decays (Fig. 2 and Table II) in contrast to the decays to the  $K^\pi = 0_1^+$  ground state band of  $^{20}\text{Ne}$ . This is consistent with a transition between shape isomeric states in  $^{24}\text{Mg}$  and  $^{20}\text{Ne}$ , i.e., 12p-4h to 8p-4h states, by emission of four nucleons in the  $(f, p)$  shell.

On a related point, many of the states in  $^{20}\text{Ne}^*$ , shown in Fig. 2, which are strongly populated from the  $^{12}\text{C} + ^{12}\text{C}$  resonances, also have preferred  $\alpha$  decays to excited states in  $^{16}\text{O}$  and substantial  $^8\text{Be} + ^{12}\text{C}$  cluster decays, indicating further evidence for their 8p-4h character. From Tables II and IV, the sum of the purely resonant parts  $\sigma_{\text{res}}(i)$  of

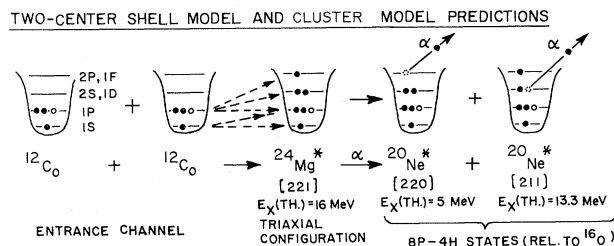


FIG. 9. An explanation for the  $^{12}\text{C} + ^{12}\text{C}$  resonances and the enhanced  $\alpha + ^{20}\text{Ne}^*$  decays from them in terms of the configurations of the two-center shell model of Chandra and Mosel (Ref. 25) and the  $(np-mh)$  configuration of Arima *et al.* (Ref. 32). In  $^{24}\text{Mg}$ , the (12p-4h) configuration is the expected eigenstate in the secondary energy minimum of the  $^{24}\text{Mg}$  potential energy surface, corresponding to a triaxial shape isomer predicted by Ragnarsson *et al.* (Ref. 27) and Leander and Larsson (Ref. 26). Arima *et al.* (Ref. 32) estimated the energies of these configurations in  $^{24}\text{Mg}$  and  $^{20}\text{Ne}$ . In  $^{24}\text{Mg}$ , the [221] energy is calculated to be at  $E_x = 15.4$  MeV +  $V$ , where  $V < 1$  MeV is the interaction of an  $N=$ three quartet and  $N=$ one quartet hole. This is very close to  $E_x = 18$  MeV which appears to be the  $0^+$  threshold for  $^{12}\text{C} + ^{12}\text{C}$  intermediate structures. In  $^{20}\text{Ne}$  the [220] and [211] states would have favored  $\alpha$  decays from  $^{24}\text{Mg}$  [221]. Their estimated energies are  $E_x = 5.1$  and  $13.3$  MeV +  $V$ , respectively. These are close to the band heads for bands which are strongly populated in the present  $^{12}\text{C}(^{12}\text{C}, \alpha)^{20}\text{Ne}^*$  resonance reaction. The [220] states in  $^{20}\text{Ne}$  correspond to the triaxial shape isomer in  $^{20}\text{Ne}$  analogous to the similar one in  $^{24}\text{Mg}$  and Leander and Larsson (Ref. 26), as discussed in the text.

the  $^{12}\text{C}(^{12}\text{C},\alpha)^{20}\text{Ne}^*(i)$  reaction as observed here are 115 and 100 mb for the  $E_{\text{c.m.}}=19.3$  and 20.3 MeV resonances, respectively. Kolata *et al.*<sup>7</sup> measured resonant  $^{16}\text{O}^*(\gamma)$  yields, which include all decays ending in  $\gamma(3_1^-, 0_2^+) \rightarrow 0_1^+$  decays, and from their data shown in Fig. 3 we estimate the purely resonant part of that cross section to be 100 and 120 mb at  $E_{\text{c.m.}}=19.3$  and 20.3 MeV, respectively. As the dominant  $^{12}\text{C}(^{12}\text{C},\alpha)^{20}\text{Ne}$  resonant yields are being accounted for in Tables II and IV, and the resonant yields directly to  $^{16}\text{O}^*$  via the reaction  $^{12}\text{C}(^{12}\text{C},^8\text{Be})^{16}\text{O}^*$  are known to be relatively small, it is concluded that the strongly resonant  $^{20}\text{Ne}^*$  states seen here decay to excited states of  $^{16}\text{O}^*$  rather than to  $^{16}\text{O}_{\text{g.s.}}$ . Hindi *et al.*<sup>30</sup> have made related observations for several of the  $^{20}\text{Ne}^*$  states studied here by directly measuring their cluster decays. The 18.54 MeV,  $J^\pi=8^+$  state has large reduced widths to  $\alpha+^{16}\text{O}^*[6.05(0^+)+6.13(3^-)]$ ,  $\alpha+^{16}\text{O}^*[6.92(2^+)+7.12(1^-)]$ , and  $^8\text{Be}+^{12}\text{C}$  channels, suggesting that it has 8p-4h structure and that the two alpha particles outside the  $^{12}\text{C}$  core are correlated. Their data also show that the  $E_x=15.9, 17.3, 20.5,$  and 24.4 MeV states in  $^{20}\text{Ne}$  have large reduced widths to  $\alpha+^{16}\text{O}^*[6.05(0^+)+6.13(3^-)]$  and  $^8\text{Be}+^{12}\text{C}$  channels, and thus may also have large 8p-4h cluster components. All of these  $^{20}\text{Ne}^*$  states have strong resonant  $\alpha$  decays

from the present  $^{12}\text{C}(^{12}\text{C},\alpha)^{20}\text{Ne}$  data supporting the shape-isomer hypothesis. It is noted, furthermore, that Leander and Larsson<sup>26</sup> predict 4p-4h excited states in  $^{16}\text{O}$  from the deformed shell model in the range below 10 MeV, and thus it is plausible that the  $^{20}\text{Ne}^* \rightarrow \alpha + ^{16}\text{O}^*$  decay is a sequential shape-isomeric transition analogous to the  $^{24}\text{Mg} \rightarrow \alpha + ^{20}\text{Ne}^*$  resonant decays that feed them. This is illustrated in Fig. 10 and lends some support for the notion of a sequence of  $\alpha$  decays between a family of cluster states.

There are some examples of  $^{12}\text{C}(^{12}\text{C},\alpha)^{20}\text{Ne}^*$  transitions that are not easily fit into the above picture. Hindi *et al.*<sup>30</sup> predict, on the basis of decay data, that a possible 8p-4h band ( $K^\pi=0_6^+$ ) may exist at higher energies with members at  $E_x(J^\pi)=12.44((0^+))$ , 15.16( $6^+$ )), and 18.54( $8^+$ ) MeV; although the  $2^+$  and  $4^+$  members have not yet been found. The 15.16 and 18.54 MeV states have large  $\alpha+^{16}\text{O}^*$  reduced widths, and the 18.54 MeV state has large  $^8\text{Be}+^{12}\text{C}$  reduced width. The 18.54( $8^+$ ) MeV state is the only one of these states with strong resonant decay here. The 12.44( $0^+$ ) MeV state should have low  $\alpha$  penetration factors over the present range, but there is no kinematic restriction on observing the 15.16( $6^+$ ) MeV state over the range of our measurements. Another indeterminate example is the assumed  $K^\pi=0_2^+$  band dis-

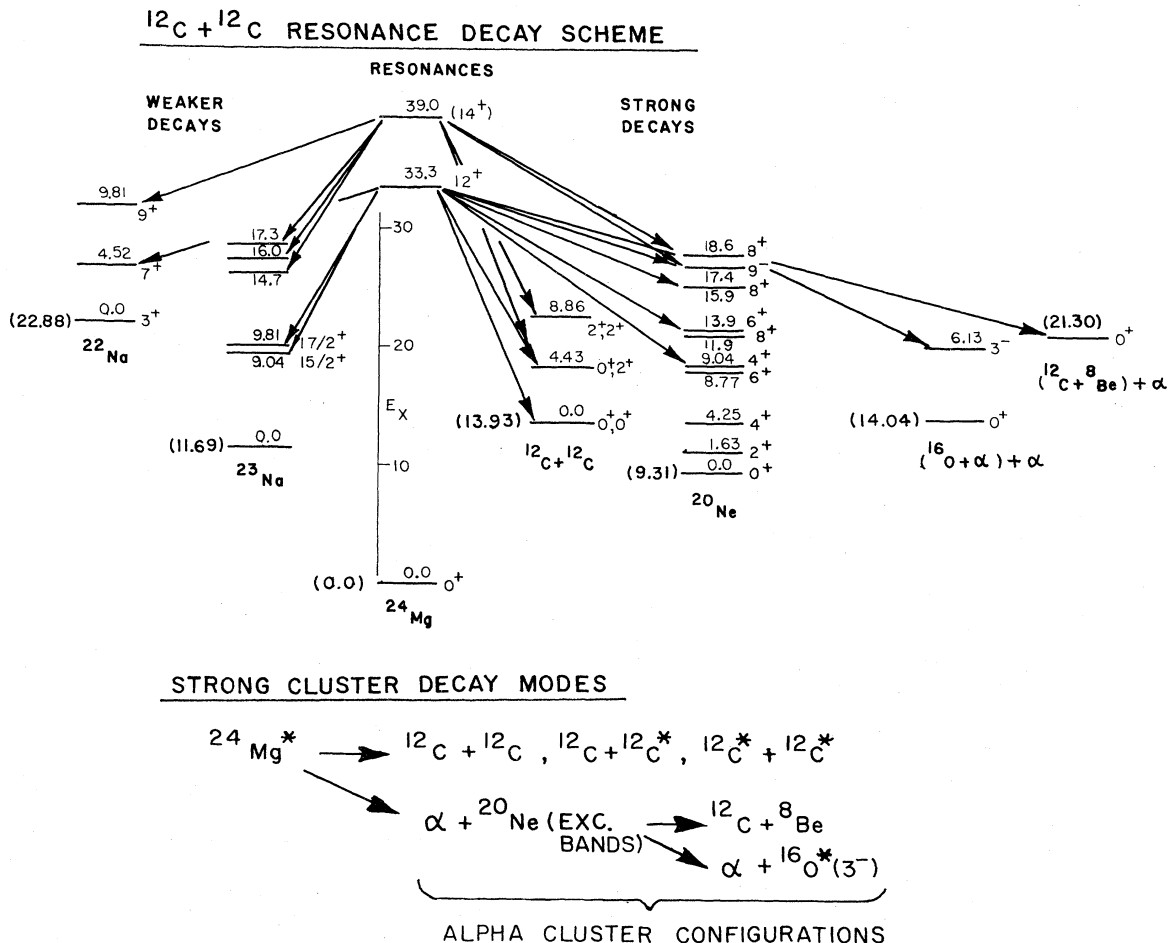


FIG. 10. A decay scheme of two  $^{12}\text{C}+^{12}\text{C}$  resonances, and their characterization as alpha-cluster transitions.

cussed by Hindi *et al.*,<sup>30</sup> Fortune *et al.*,<sup>33</sup> Middleton *et al.*,<sup>29</sup> and Greenwood *et al.*,<sup>19</sup> with members at  $E_x(J^\pi)=6.72(0^+)$ ,  $7.42(2^+)$ ,  $9.99(4^+)$ ,  $13.93(6^+)$ , and  $20.5((8^+))$  MeV. This band is thought to have predominant  $(sd)^4$  shell structure, and is not thought to be of pure 8p-4h character.<sup>33,29,30</sup> Yet Voit *et al.*<sup>22</sup> observed enhanced resonant cross sections to it relative to the ground band from  $^{12}\text{C}(^{12}\text{C},\alpha)^{20}\text{Ne}$  near the Coulomb barrier. We also observe strong decays to the  $13.93(6^+)$  MeV state and to the tentative 20.5 MeV band member, but a much weaker decay to the  $9.99(4^+)$  MeV member compared to the  $9.04(4^+)$  MeV member of the  $K^\pi=0_3^+$  band. Because the data<sup>22</sup> of Voit *et al.* and much of ours are single angle data, no firm reduced widths can be extracted; however, generally the  $K^\pi=0_2^+$  (6.72 MeV) band is more weakly populated than the  $K^\pi=0_3^+$  (7.2 MeV) band, supporting the claim that the latter is a purer 8p-4h band. As Fortune *et al.*,<sup>33</sup> Hindi *et al.*,<sup>30</sup> and others cite, the  $K^\pi=0_2^+$  band certainly has considerable admixtures, and, from the facts given here, these admixtures might include 8p-4h structures. These examples do not contradict the hypothesis of the shape isomeric transitions. Rather they may indicate that configuration admixture may spread the shape-isomeric 8p-4h strength in  $^{20}\text{Ne}$  over many states, analogous to the fragmentation of the shape isomeric states in  $^{24}\text{Mg}$  mentioned above.

#### IV. CONCLUSION

Measurements of excitation functions for the  $^{12}\text{C}(^{12}\text{C},\alpha)^{20}\text{Ne}^*$  reaction over a wide energy range ( $E_{\text{c.m.}}=14\text{--}40$  MeV) reveal the existence of prominent intermediate structure resonances which are correlated with resonances in other channels, and which selectively and nonstatistically decay to special  $^{20}\text{Ne}^*$  states. Angular distributions have also been measured over three intermediate structure resonances  $E_{\text{c.m.}}=18.4$ ,  $19.3$ , and  $20.3$  MeV, and reduced widths have been extracted for many  $\alpha+^{20}\text{Ne}^*$  final states. It is found that reduced widths for decay to a few special  $^{20}\text{Ne}$  states, some of which are known to have 8p-4h configurations, are an order of magnitude larger than reduced widths for decay to members of the ground state rotational band. Moreover, the reduced widths for alpha decay to some of these special  $^{20}\text{Ne}^*$  states are comparable to those for the elastic and inelastic channel. The existence of  $^{24}\text{Mg}$  shape isomeric states in a deformed shell model secondary potential minimum presents a possible explanation for  $^{12}\text{C}+^{12}\text{C}$  resonances and their nonstatistical decays to  $^{20}\text{Ne}$ .

#### ACKNOWLEDGMENTS

We thank Professor Arthur Kerman for helpful support and discussions. This work was supported by the U.S. Department of Energy under Contract No. AC02-76ER03069.

\*Present address: Instituto de Física, Universidade de São Paulo, São Paulo, Brazil.

- <sup>1</sup>E. Almqvist, D. A. Bromley, and J. A. Kuehner, *Phys. Rev. Lett.* **4**, 515 (1960).
- <sup>2</sup>D. A. Bromley, J. A. Kuehner, and E. Almqvist, *Phys. Rev. Lett.* **4**, 365 (1960); *Phys. Rev.* **123**, 878 (1961); E. Almqvist *et al.*, *ibid.* **130**, 1140 (1963).
- <sup>3</sup>G. J. Michaud and E. W. Vogt, *Phys. Rev. C* **5**, 350 (1972).
- <sup>4</sup>E. R. Cosman, K. Van Bibber, T. M. Cormier, T. N. Chia, A. Sperduto, and O. Hansen, in *Proceedings of the International Conference on Nuclear Physics, Munich, 1973*, edited by J. de Boer and H. J. Mang (North-Holland, Amsterdam, 1973), p. 542; K. Van Bibber, E. R. Cosman, A. Sperduto, T. M. Cormier, T. N. Chin, and O. Hansen, *Phys. Rev. Lett.* **32**, 687 (1974).
- <sup>5</sup>E. R. Cosman, T. M. Cormier, K. Van Bibber, A. Sperduto, G. Young, J. Erskine, L. R. Greenwood, and O. Hansen, *Phys. Rev. Lett.* **35**, 265 (1975).
- <sup>6</sup>P. Sperr, T. H. Braid, Y. Eisen, D. G. Kovar, F. W. Prosser, Jr., J. P. Schiffer, S. L. Tabor, and S. Vigdor, *Phys. Rev. Lett.* **37**, 321 (1976).
- <sup>7</sup>J. J. Kolata, R. M. Freeman, F. Haas, B. Heusch, and A. Gallman, *Phys. Rev. C* **21**, 579 (1980).
- <sup>8</sup>T. M. Cormier, J. Applegate, G. M. Berkowitz, P. Braun-Munzinger, T. M. Cormier, J. W. Harris, C. M. Jachinski, L. L. Lee, Jr., J. Barrette, and H. E. Wegner, *Phys. Rev. Lett.* **38**, 940 (1977); T. M. Cormier *et al.*, *ibid.* **40**, 924 (1978).
- <sup>9</sup>H. Emling, R. Nowotny, D. Pelte, and G. Schrieder, *Nucl. Phys.* **A211**, 600 (1975); H. Emling, R. Nowotny, D. Pelte, G. Schrieder, and W. Weidenmeier, *ibid.* **A239**, 172 (1975).
- <sup>10</sup>N. R. Fletcher, J. D. Fox, G. J. Kekelis, G. R. Morgan, and G. A. Norton, *Phys. Rev. C* **13**, 1175 (1976); D. R. James and N. R. Fletcher, *ibid.* **17**, 2248 (1978).

- <sup>11</sup>A. Arima, G. Scharff-Goldhaber, and K. W. McVoy, *Phys. Lett.* **40B**, 7 (1972).
- <sup>12</sup>B. Imanishi, *Nucl. Phys.* **A125**, 33 (1969); T. Matsuse, Y. Kondō, and Y. Abe, *Prog. Theor. Phys.* **59**, 1009 (1978); T. Matsuse *et al.*, *ibid.* **59**, 1904 (1978); Y. Kondō, Y. Abe, and T. Matsuse, *Phys. Rev. C* **19**, 1356 (1979).
- <sup>13</sup>W. Scheid, W. Greiner, and R. Lemmer, *Phys. Rev. Lett.* **25**, 176 (1970); H. J. Fink, W. Scheid, and W. Greiner, *Nucl. Phys.* **A188**, 259 (1972).
- <sup>14</sup>H. Feshbach, *J. Phys. (Paris)* **C5**, 177 (1976); H. Feshbach, MIT Internal Report, CTP No. 671, 1977.
- <sup>15</sup>K. A. Erb and D. A. Bromley, *Phys. Rev. C* **23**, 2781 (1981); F. Iachello, *ibid.* **23**, 2778 (1981).
- <sup>16</sup>R. L. Phillips, K. A. Erb, D. A. Bromley, and J. Weneser, *Phys. Rev. Lett.* **42**, 566 (1979).
- <sup>17</sup>D. Shapira, R. G. Stokstad, and D. A. Bromley, *Phys. Rev. C* **10**, 1063 (1974).
- <sup>18</sup>E. Almqvist, J. A. Kuehner, D. McPherson, and E. W. Vogt, *Phys. Rev.* **136**, 884 (1964).
- <sup>19</sup>L. R. Greenwood, R. E. Segel, K. Raghunathan, M. A. Lee, H. T. Fortune, and J. R. Erskine, *Phys. Rev. C* **12**, 156 (1975).
- <sup>20</sup>D. Evers, in *Resonances in Heavy-Ion Reactions*, edited by K. A. Eberhard (Springer, Berlin, 1982), p. 53.
- <sup>21</sup>E. R. Cosman, R. Ledoux, and A. J. Lazzarini, *Phys. Rev. C* **21**, 2111 (1980).
- <sup>22</sup>H. Voit, W. Galster, W. Treu, H. Frölich, and P. Dück, *Phys. Lett.* **67B**, 399 (1977).
- <sup>23</sup>E. R. Cosman, R. J. Ledoux, M. J. Bechara, C. E. Ordoñez, and H. A. Al-Juwair, in *Resonances in Heavy-Ion Reactions*, edited by K. A. Eberhard (Springer, Berlin, 1982), p. 112.
- <sup>24</sup>R. J. Ledoux, M. J. Bechara, C. E. Ordoñez, H. A. Al-Juwair, and E. R. Cosman, *Phys. Rev. C* **27**, 1103 (1983).
- <sup>25</sup>H. Chandra and U. Mosel, *Nucl. Phys.* **A239**, 151 (1978).

- <sup>26</sup>G. Leander and S. E. Larsson, Nucl. Phys. **A239**, 93 (1975).
- <sup>27</sup>I. Ragnarsson, S. Åberg, and R. K. Sheline, Phys. Scr. **24**, 215 (1981).
- <sup>28</sup>U. Mosel, in *Resonances in Heavy-Ion Reactions*, edited by K. A. Eberhard (Springer, Berlin, 1982), p. 358.
- <sup>29</sup>R. Middleton, J. D. Garrett, and H. T. Fortune, Phys. Rev. Lett. **27**, 950 (1971); R. Middleton *et al.*, J. Phys. (Paris) **C6**, 7 (1971).
- <sup>30</sup>M. M. Hindi, J. H. Thomas, D. C. Radford, and P. D. Parker, Phys. Lett. **99B**, 33 (1981); M. M. Hindi *et al.*, Phys. Rev. C **27**, 2902 (1983).
- <sup>31</sup>H. Voit, G. Ischenko, and F. Siller, Phys. Rev. Lett. **30**, 564 (1973).
- <sup>32</sup>A. Arima, V. Gillet, and J. Ginocchio, Phys. Rev. Lett. **25**, 1043 (1970).
- <sup>33</sup>H. T. Fortune, R. Middleton, and R. R. Betts, Phys. Rev. Lett. **29**, 738 (1972).